Deep Convection and Cirrus Anvils in CRM RCE Simulations

Susan C. van den Heever
Colorado State University
Fort Collins, CO

Image: Astronaut Alex Gerst on September 8, 2014, from the International Space Station.

Radiative Convective Equilibrium (RCE) Simulations

- RAMS model (Cotton et al 2003; Saleeby and van den Heever 2013)
- High spatial (Δx=Δy=500m) and temporal resolution (minutes)
- Long duration (50-60 days)
- Sophisticated microphysics, radiation and land surface parameterization schemes

Disturbed and Undisturbed Regions

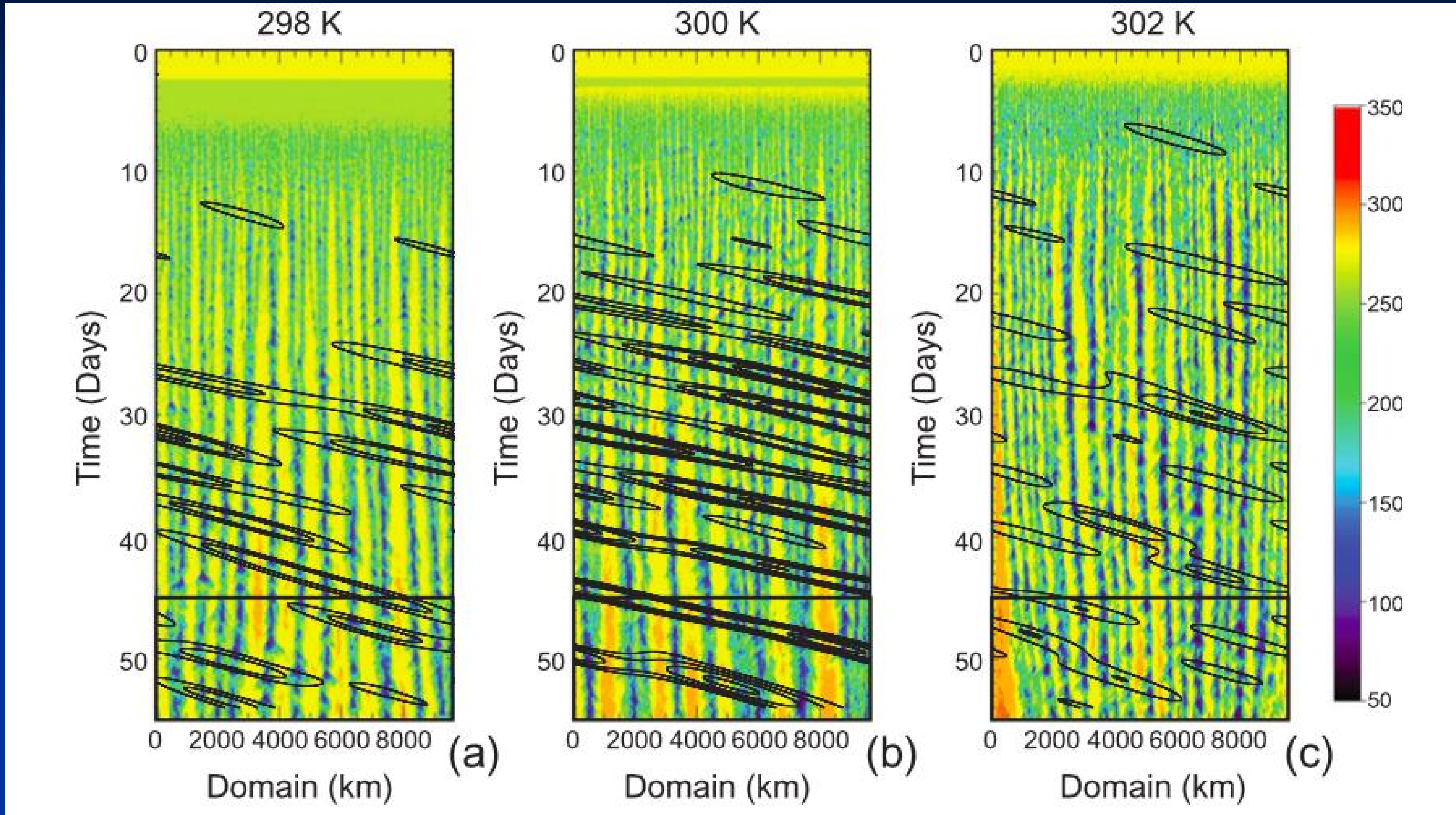

Hovmoller plots of OLR as a function of SST. Black contour lines denote filtered OLR anomalies corresponding to equatorial Kelvin waves.

Organization varies as a function of SST

After Posselt, van den Heever, Stephens and Igel 2012 J. Clim

RCE Animations

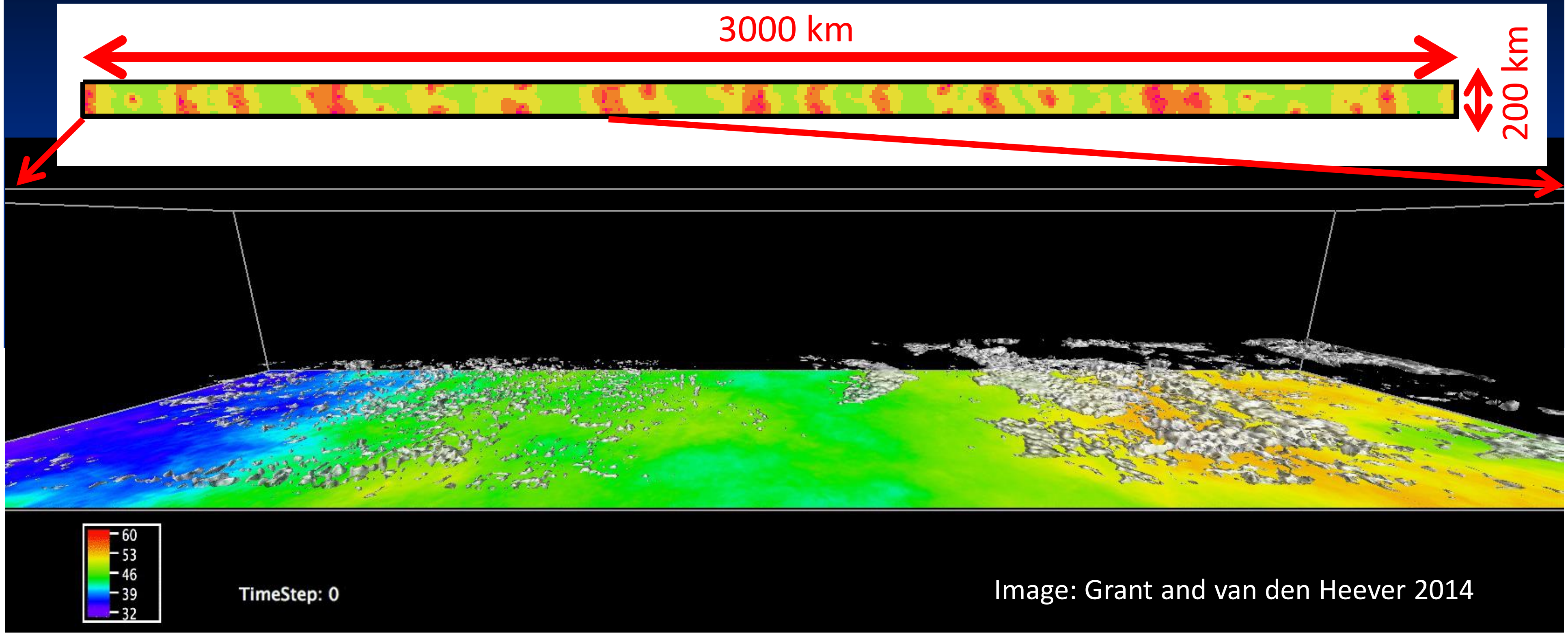

A portion (left 1/3) of an RCE simulation: 1000 by 200 by 25 km for 5 days (66 through 71) at hourly intervals. Shading represents precipitable water (mm); white is a total condensate isosurface of 0.4 g/kg

- Trimodal distribution of convection – shallow, congestus and deep convective modes

Use of RCE Simulations

- Convective and stratiform dynamical and precipitation characteristics as a function of SST
- Anvil – pedestal (updraft) relationships
- Latent heating characteristics and processes
- Environmental impacts on anvil characteristics

Use of RCE Simulations

- Convective and stratiform dynamical and precipitation characteristics as a function of SST
- Anvil – pedestal (updraft) relationships
- Latent heating characteristics and processes
- Environmental impacts on anvil characteristics

Posselt, van den Heever, Stephens and Igel 2012 J. Clim

TABLE 1. Means of cloud, radiation, and vertical mass flux variables averaged over the entire domain and for the last 10 days of each simulation.

	SST		
	298 K	300 K	302 K
Mean PW, full domain (kg m^{-2})	29.34	38.00	48.20
Mean precipitation rate (mm h^{-1})	2.199	2.384	2.485
Mean OLR, full domain (W m^{-2})	245.04	241.27	240.59
High cloud fraction (%)	33.65	36.31	37.41
Mean TWP, full domain (g m^{-2})	96.14	96.54	91.90
Mean LWP, full domain (g m^{-2})	33.81	38.08	38.11
Mean IWP, full domain (g m^{-2})	62.33	58.45	53.79
Mean vertical mass flux: Disturbed regions (kg m^{-2} s^{-1})	0.154	0.125	0.104
Mean vertical mass flux: Undisturbed regions (kg m^{-2} s^{-1})	−0.095	−0.090	−0.076
Mean surface wind speed (m s^{-1})	1.62	1.58	1.33

- With increasing SST
  - Enhanced precipitation rates
  - Increased high cloud fraction
  - Increased mean TWP but reduced mean IWP

Posselt, van den Heever, Stephens and Igel 2012 J. Clim

TABLE 2. As in Table 1 but for statistics describing changes in convective intensity with SST.

	SST		
	298 K	300 K	302 K
Mean w where w > 1	2.665	2.906	3.042
Percent of domain with w > 1 m s^{-1}	1.047%	0.791%	0.783%
Percent of domain with w > 10 m s^{-1}	0.025%	0.032%	0.039%
Percent of domain with precipitation > 250 mm day^{-1}	0.197%	0.212%	0.234%
Percent of domain containing cold pools	2.32	3.38	4.83
Mean temperature perturbation in cold pools (K)	−1.12	−1.15	−1.10
Precipitation rate in cold pools (mm h^{-1})	9.01	9.63	10.15
Percent of precipitation falling in cold pools	79.58%	74.87%	86.00%
Mean convective mass flux (kg m^{-2} s^{-1})	4.881	4.085	3.797
Mean stratiform mass flux (kg m^{-2} s^{-1})	0.043	0.030	0.021
Percent of precipitation in convective regions	30.42%	29.18%	35.87%
Percent of precipitation in stratiform regions	66.22%	67.66%	61.06%

- With increasing SST
  - Greater mean W
  - Less frequent moderate updrafts, more frequent very strong updrafts
  - Shifts to more convective, less stratiform type precipitation

Posselt, van den Heever, Stephens and Igel 2012 J. Clim

TABLE 4. As in Table 1 but for results of the four-class partitioning scheme.

	SST		
	298 K	300 K	302 K
Percent deep convective cores	0.732	0.719	0.693
Percent shallow convective	6.113	5.767	5.015
Percent precipitating stratiform	2.987	3.758	2.804
Percent nonprecipitating stratiform	25.645	28.513	29.212
Deep convective precipitation rate	210.848	232.255	269.543
Shallow convective precipitation rate	2.406	3.038	3.707
Precipitating stratiform precipitation rate	18.588	15.965	17.760
Deep convective precipitation fraction	68.025	67.797	72.727
Shallow convective precipitation fraction	6.520	7.127	7.272
Precipitating stratiform precipitation fraction	24.241	24.126	19.426
Deep convective vertical velocity (cloudy, $w > 0$)	0.842	0.821	0.900
Shallow convective vertical velocity (cloudy, $w > 0$)	0.089	0.099	0.105
Precipitating stratiform vertical velocity (cloudy, $w > 0$)	0.132	0.113	0.128

- With increasing SST
  - Reduced number of deep convective cores but these cores precipitate more heavily
  - Convective updrafts are enhanced
  - Non-precipitating stratiform anvils cover more area

Use of RCE Simulations

- Convective and stratiform dynamical and precipitation characteristics as a function of SST
- Anvil – pedestal (updraft) relationships
- Latent heating characteristics and processes
- Environmental impacts on anvil characteristics

Anvil – Pedestal (Updraft) Relationship CloudSat Data

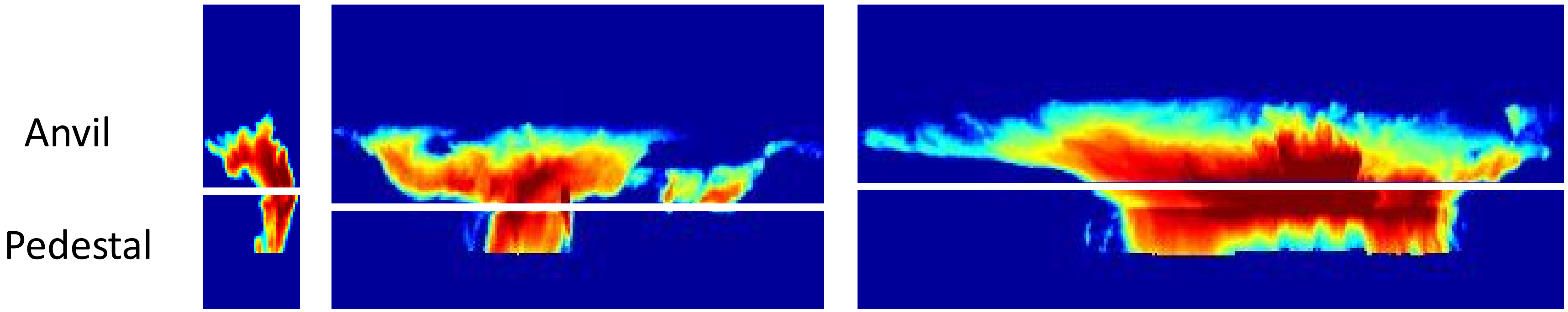

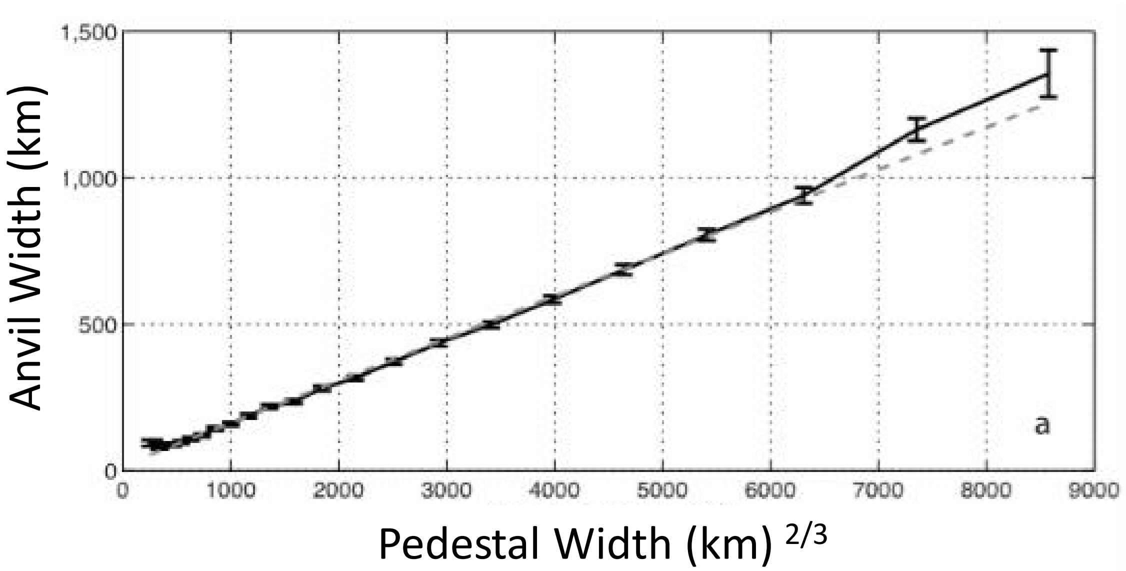

The black solid line illustrates the mean anvil width binned by pedestal width. Error bars show the 95% confidence interval for the mean. The gray dashed line shows the linear best fit to the data. Note that the abscissa is pedestal width to the 2/3 power. (after Igel and van den Heever, 2015)

Anvil-Pedestal (Updraft) Relationship
RCE Simulation

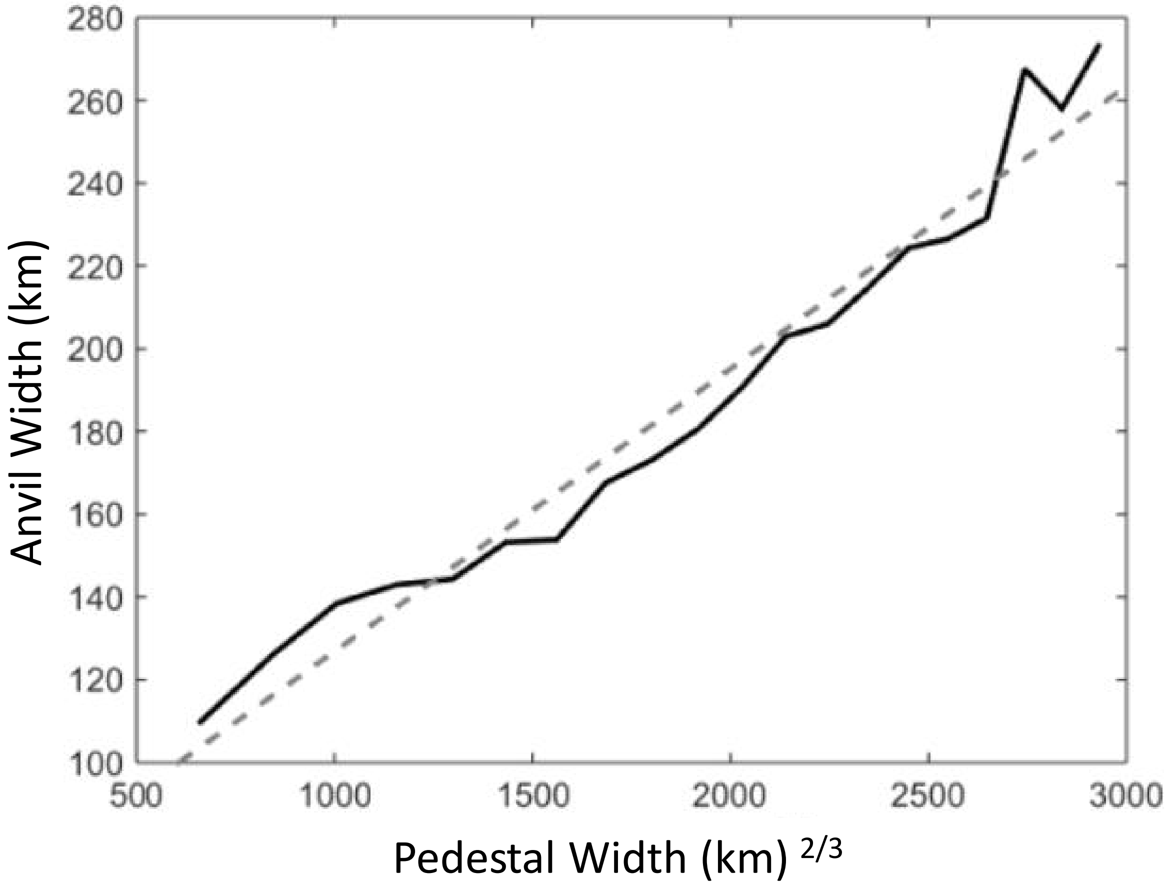

Mean anvil width as a function of binned pedestal width to the 2/3rd power in black. A linear fit is shown in the gray dashed line (after Igel and van den Heever, 2015)

Use of RCE Simulations

- Convective and stratiform dynamical and precipitation characteristics as a function of SST
- Anvil – pedestal (updraft) relationships
- Latent heating characteristics and processes
- Environmental impacts on anvil characteristics

Linear Convection in RCE Simulations

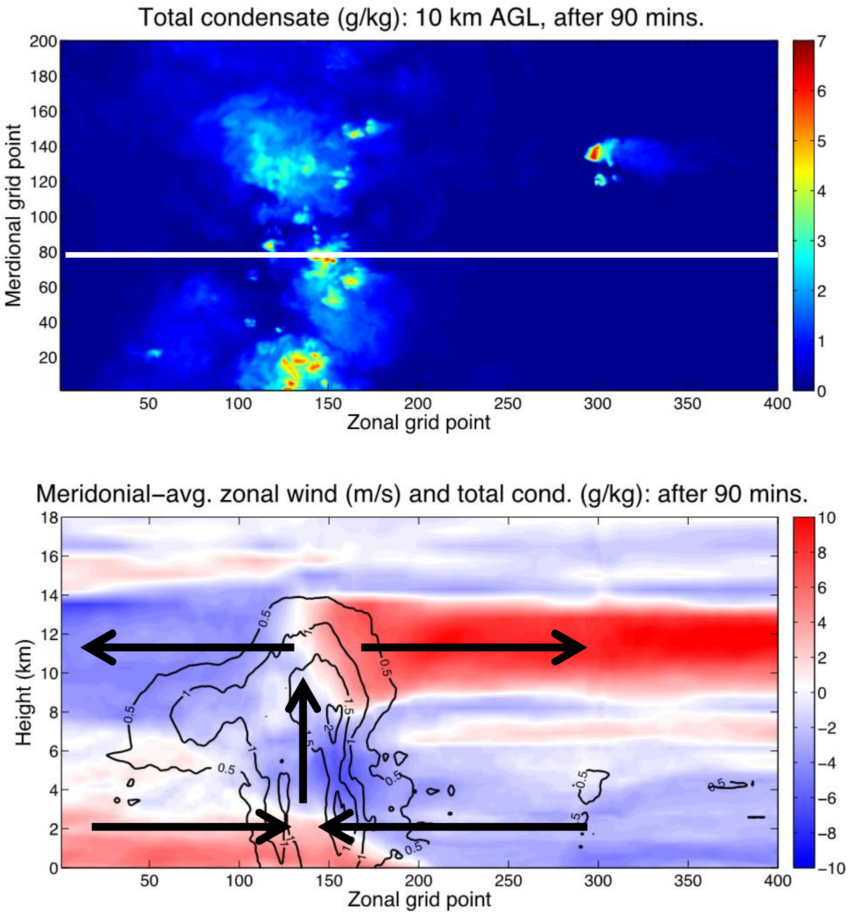

Å Tropical squall lines evident in RCE simulations (the figure shows a zoomed in portion of the domain; grid spacing of 250m)

Å Cross section showing zonal flow through convective line

McGee and van den Heever 2014 JAS

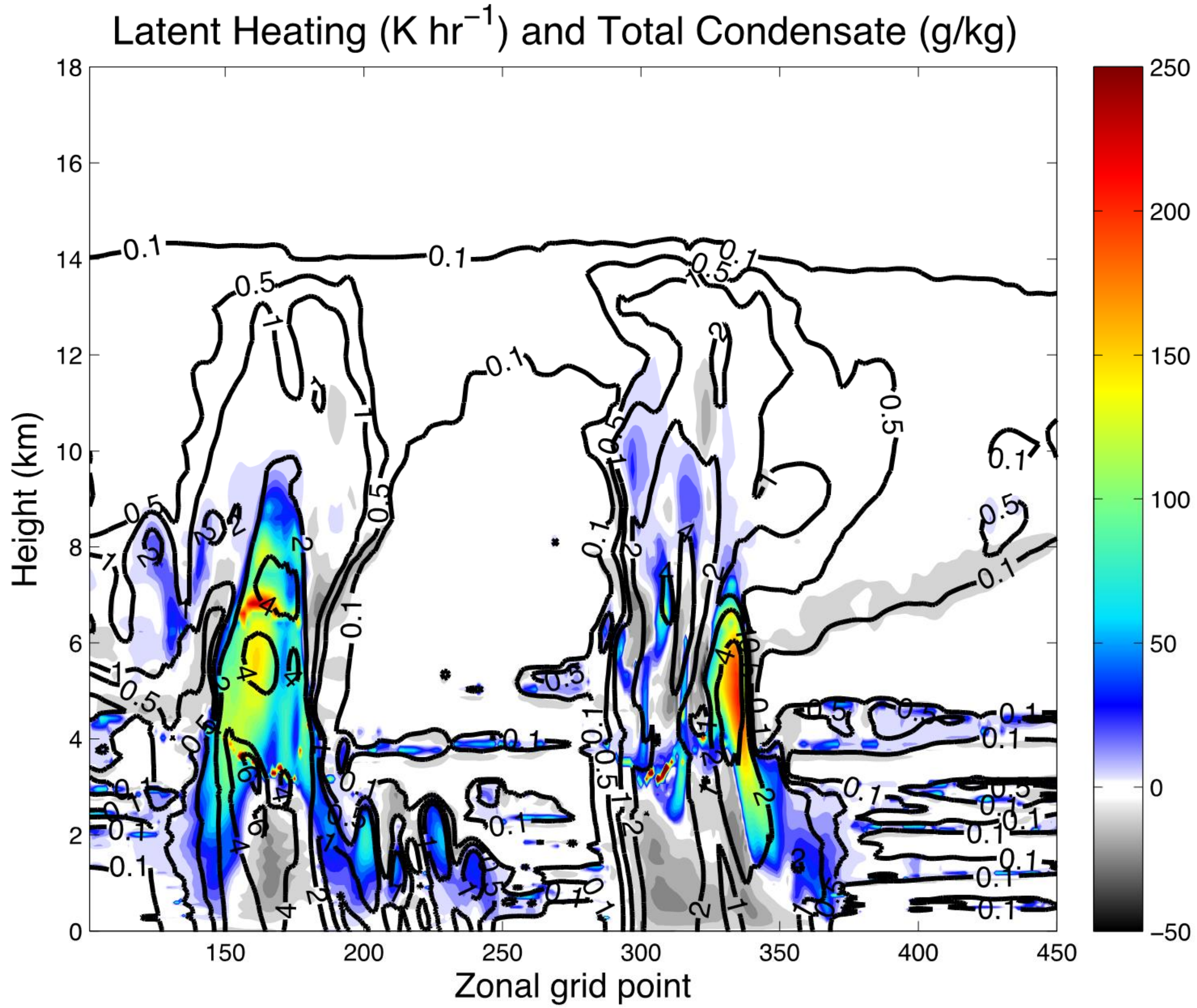

Cross-section after 45 minutes taken from a portion of the inner grid of a simulation that nests down to 250 meter grid spacing within RCE model output of tropical deep convection; shading is latent heating rate (K hr^{-1}) and contours are total condensate (g/kg). Latent heating rates are calculated from microphysical budget terms tracked within RAMS.

Vertical Transport

Animation of a trajectory through the Tropical Squall Line

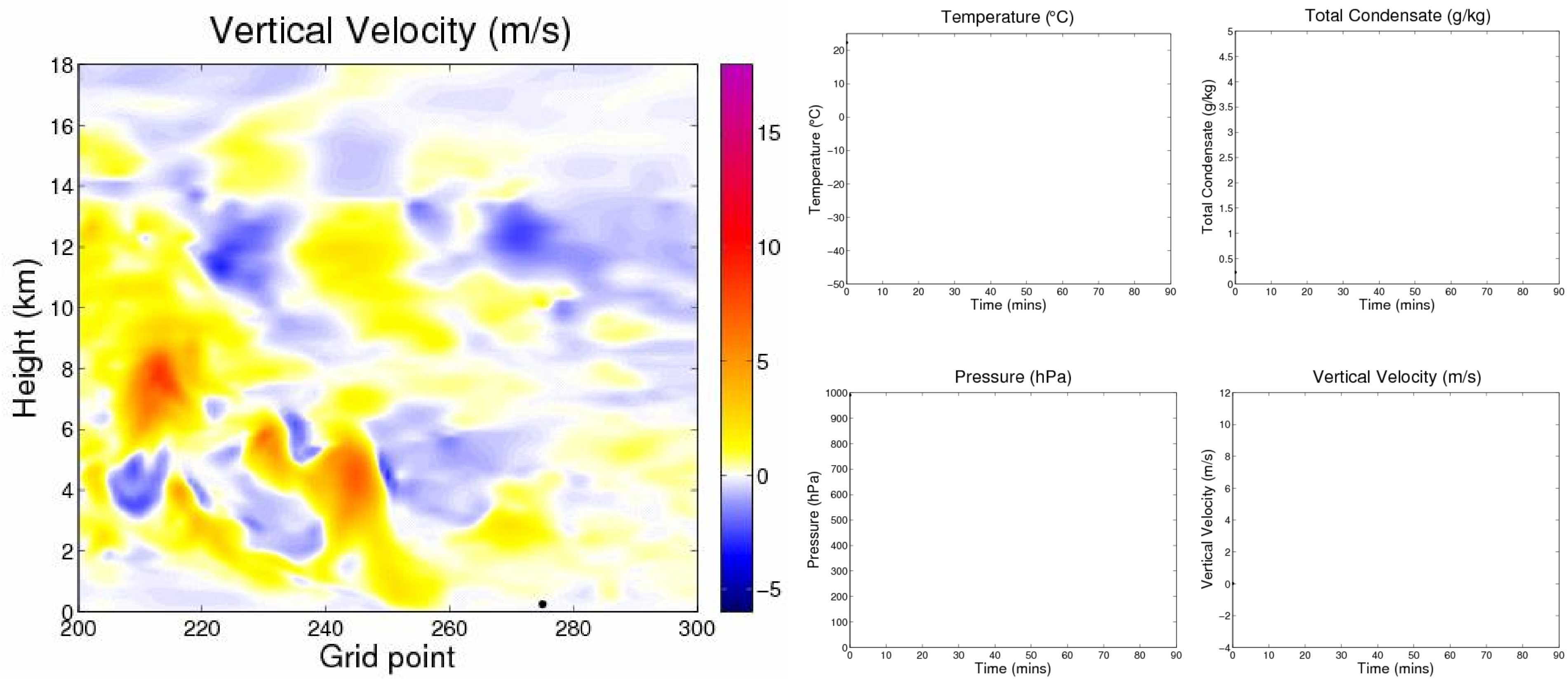

McGee and van den Heever 2014 JAS

Trajectories

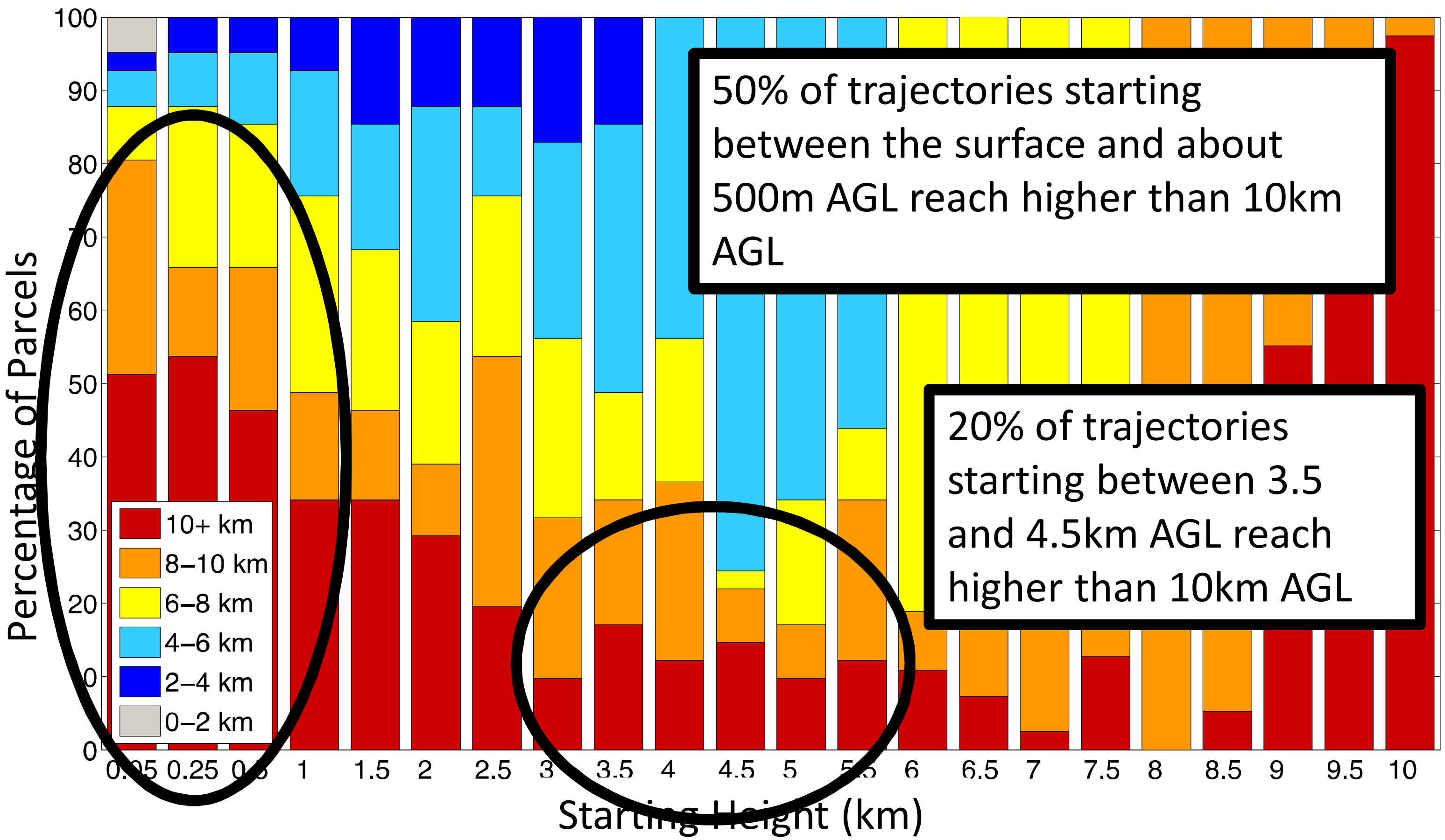

Distribution of maximum trajectory heights by starting altitude for forward trajectories (after McGee and van den Heever 2014)

Along Trajectory Latent Heating

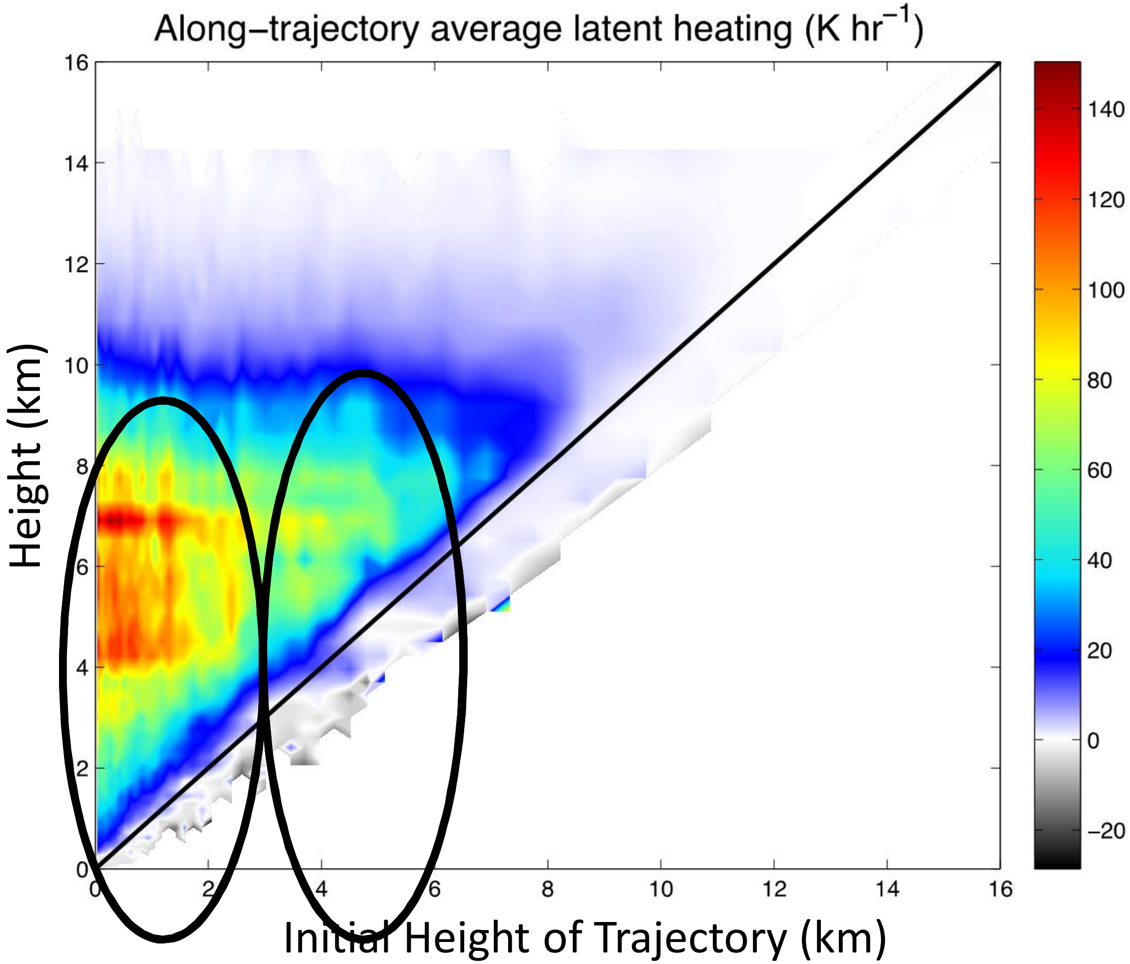

- Å Parcels originating from the boundary layer have the highest average latent heating rates
- Å Entrained mid-level inflow air also plays a role in latent heating

For back-trajectories that end in the deep convective core in the upper troposphere, plot shows average along-trajectory latent heating rates as functions of trajectory ***initial height*** (x-axis) in the ambient inflow environment and the ***height at some time later*** (y-axis).

Latent Heating Rates due to Various Processes

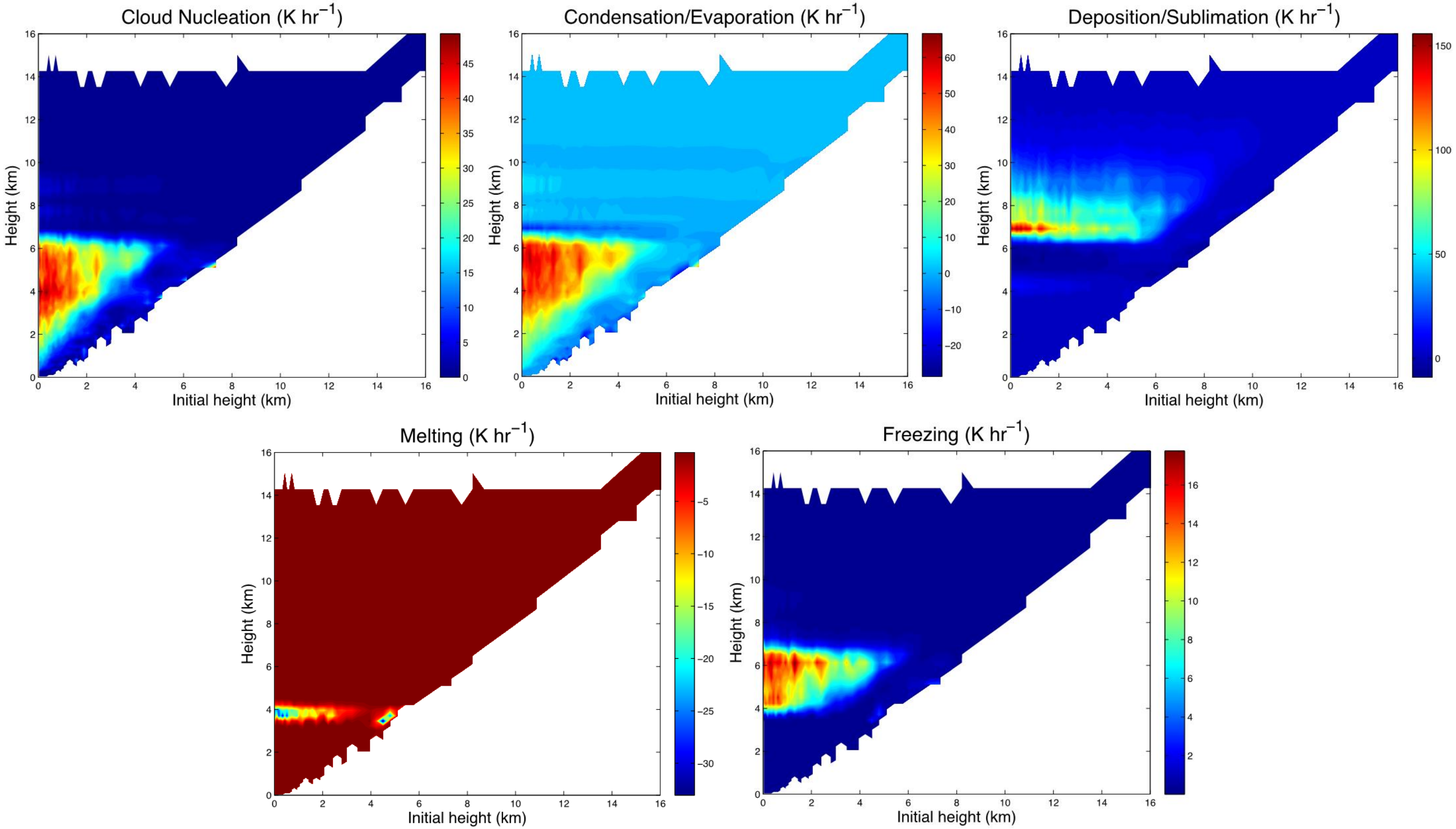

Average latent heating rates along back-trajectories that after 90 minutes are above 10 km and co-located with total condensate > 1 g/kg (after McGee and van den Heever 2014)

Use of RCE Simulations

- Convective and stratiform dynamical and precipitation characteristics as a function of SST
- Anvil – pedestal (updraft) relationships
- Latent heating characteristics and processes
- Environmental impacts on anvil characteristics

Environmental Impacts on Anvils - CloudSat

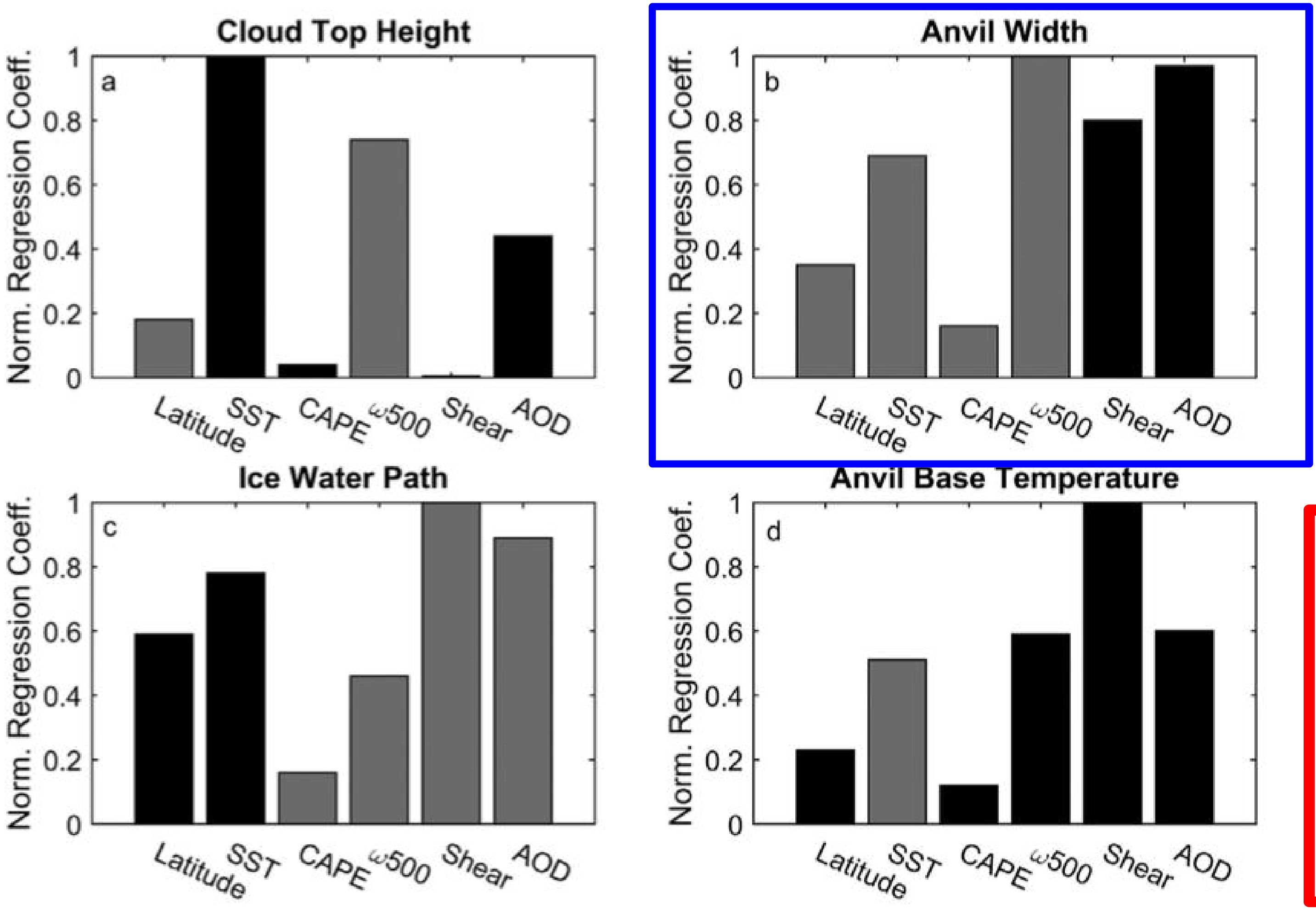

For example, anvil width is most impacted by vertical motion at 500mb, shear and AOD

Are these relationships evident in RCE simulations? If so, what PROCESSES cause such relationships?

Normalized multiple linear regression coefficients for each predictor (each bar) for various cloud characteristics. The gray bars indicate negative values (after Igel and van den Heever 2015, JGR)